Prominent Mitochondrial Injury as an Early Event in Heme Protein-Induced Acute Kidney Injury

Raman Deep Singh [iD],[1] Anthony J. Croatt,[1] Allan W. Ackerman,[1] Joseph P. Grande [iD],[2] Eugenia Trushina [iD],[3,4] Jeffrey L. Salisbury,[5,6] Trace A. Christensen,[5] Christopher M. Adams,[7] Tamara Tchkonia,[8] James L. Kirkland,[8,9] and Karl A. Nath [iD][1]

Key Points

- In heme protein–induced AKI, mitochondrial functional integrity, as reflected by ATP and NAD^+ content and NAD^+/NADH ratio, is impaired.
- Mitochondrial quality control is compromised as reflected by impaired biogenesis, exaggerated fission, and marked ultrastructural damage.
- Modern concepts regarding mitochondria and AKI apply to heme protein–induced AKI, with the possibility of novel therapeutic strategies.

Abstract

Background Mitochondrial injury occurs in and underlies acute kidney injury (AKI) caused by ischemia-reperfusion and other forms of renal injury. However, to date, a comprehensive analysis of this issue has not been undertaken in heme protein–induced AKI (HP-AKI). We examined key aspects of mitochondrial function, expression of proteins relevant to mitochondrial quality control, and mitochondrial ultrastructure in HP-AKI, along with responses to heme in renal proximal tubule epithelial cells.

Methods The long-established murine glycerol model of HP-AKI was examined at 8 and 24 hours after HP-AKI. Indices of mitochondrial function (ATP and NAD^+), expression of proteins relevant to mitochondrial dynamics, mitochondrial ultrastructure, and relevant gene/protein expression in heme-exposed renal proximal tubule epithelial cells *in vitro* were examined.

Results ATP and NAD^+ content and the NAD^+/NADH ratio were all reduced in HP-AKI. Expression of relevant proteins indicate that mitochondrial biogenesis (PGC-1α, NRF1, and TFAM) and fusion (MFN2) were impaired, as was expression of key proteins involved in the integrity of outer and inner mitochondrial membranes (VDAC, Tom20, and Tim23). Conversely, marked upregulation of proteins involved in mitochondrial fission (DRP1) occurred. Ultrastructural studies, including novel 3D imaging, indicate profound changes in mitochondrial structure, including mitochondrial fragmentation, mitochondrial swelling, and misshapen mitochondrial cristae; mitophagy was also observed. Exposure of renal proximal tubule epithelial cells to heme *in vitro* recapitulated suppression of PGC-1α (mitochondrial biogenesis) and upregulation of p-DRP1 (mitochondrial fission).

Conclusions Modern concepts pertaining to AKI apply to HP-AKI. This study validates the investigation of novel, clinically relevant therapies such as NAD^+-boosting agents and mitoprotective agents in HP-AKI.

Introduction

Caused by ischemia, heme proteins, toxins, sepsis, or urinary tract obstruction, among other insults, AKI may develop in 5%–15% of hospitalized patients and in >50% of critically ill patients in whom mortality may be >50% (1). Additionally, CKD and ESKD may ensue in subsets of patients with AKI. AKI exacts some $10 billion/year or more in health care costs (2). AKI is essentially managed by supportive care and minimizing insults. Strategies that mitigate AKI and hasten recovery are thus urgently needed.

[1]Division of Nephrology and Hypertension, Department of Medicine, Mayo Clinic Rochester, Minnesota
[2]Department of Laboratory Medicine and Pathology, Mayo Clinic Rochester, Minnesota
[3]Department of Neurology, Mayo Clinic Rochester, Minnesota
[4]Department of Molecular Pharmacology and Experimental Therapeutics, Mayo Clinic Rochester, Minnesota
[5]Microscopy and Cell Analysis Core Facility, Mayo Clinic Rochester, Minnesota
[6]Department of Biochemistry and Molecular Biology, Mayo Clinic Rochester, Minnesota
[7]Division of Endocrinology, Diabetes, Metabolism and Nutrition, Department of Medicine, Mayo Clinic Rochester, Minnesota
[8]Department of Physiology and Biomedical Engineering, Mayo Clinic Rochester, Minnesota
[9]Department of General Internal Medicine, Department of Medicine, Mayo Clinic Rochester, Minnesota

Correspondence: Dr. Karl A. Nath, Mayo Clinic, Siebens 7, 200 First St., SW, Rochester, MN 55905. Email: nath.karl@mayo.edu

A time-honored approach in AKI is the study of rodent models of AKI, which, in aggregate, have elucidated the discovery of new biomarkers of AKI, the pathogenesis of AKI, and strategies that may be the basis for novel therapies (3); for example, novel studies of such models uncovered the exciting prospects for NAD^+-boosting agents (4,5) and stem cell-based therapies (6,7) in mitigating AKI. AKI models include ischemia-reperfusion injury (IRI), heme protein–induced AKI (HP-AKI), sepsis-associated AKI, and cisplatin-induced AKI.

Models of HP-AKI are essential in aiding the understanding of AKI induced by rhabdomyolysis. However, the value of these specific models goes well beyond this disease for several reasons. First, renal heme content is increased in AKI caused by ischemia (8) and nephrotoxins that do not overtly involve heme proteins (9); a substantial body of data now suggests that heme may be one of the final common pathways for AKI, irrespective of the basis for AKI (10). Second, there is now mounting evidence that AKI in sepsis and other conditions arises at least in part from circulating cell-free hemoglobin (CFH) and an attendant increase in tissue heme (11). Third, models of HP-AKI have played a significant role in the evolution of broadly applicable concepts in AKI, including, for example, the recognition that AKI may be a precursor to CKD (12); the induction of heme oxygenase-1 and ferritin as a broad-based cytoprotective response in the kidney (13,14); the roles of hydrogen peroxide (15), lipid peroxidation (16), glutathione depletion (17), and catalytic iron in the causation of AKI (18); the vascular basis for AKI (19); the demonstration that cytochrome p450 proteins may serve as a source of iron in AKI (20); and the recognition that complement activation drives, in part, HP-AKI (21).

Some 25 years ago, we demonstrated that in a classic model of HP-AKI (glycerol-induced myolysis and hemolysis), mitochondrial respiration—assessed by state 2, 3, and 4 oxygen consumption and the respiratory control ratio, the acceptor control ratio, and the P/O ratio (ADP utilized/oxygen consumed)—was profoundly impaired 24 hours after the induction of HP-AKI (22). In the ensuing years, the knowledge of mitochondrial dynamics, biogenesis, fission, fusion, and quality control in general and of AKI in particular has exponentially increased, with the resulting appearance of entirely new paradigms for AKI (23–27). These paradigms have not been comprehensively examined in models of HP-AKI, including the glycerol-induced model of HP-AKI. Using this model of HP-AKI, we examine mitochondrial function, expression of proteins related to mitochondrial fission and fusion, and mitochondrial structure including 3D imaging, the latter essential in determining whether mitochondrial fission occurs.

Materials and Methods
Model of HP-AKI
All studies were approved by the Institutional Animal Care and Use Committee of Mayo Clinic and performed in accordance with the Guide for the Care and Use of Laboratory Animals of the National Institutes of Health. Male C57BL/6J mice (10–20 weeks of age) used for these studies were purchased from the Jackson Laboratory (Bar Harbor, ME). We used the glycerol model of HP-AKI as in our previous studies (28,29). Briefly, after 16–18 hours of dehydration, mice were anesthetized (ketamine and xylazine, 90 and 10 mg/kg, respectively, given intraperitoneally) and given an intramuscular injection of glycerol (50% in water, 6 ml/kg), one half of the dose into each anterior thigh muscle. Renal tissues were harvested at 8 and 24 hours after glycerol injection for analysis of mitochondrial function, biogenesis, dynamics, and ultrastructure.

Western Blot Analysis
Western blots were performed on whole kidney lysates and cell lysates as outlined previously (30,31). Membranes were incubated overnight at 4°C with primary antibodies against PTEN-induced kinase 1 (PINK1) and mitofusin 2 (MFN2; catalog nos. NB100–493 and NBP2–66383, respectively; Novus Biologicals, Centennial, CO); peroxisome proliferator-activated receptor gamma coactivator-1α (PGC-1α; catalog no. ab191838; Abcam, Waltham, MA); voltage-dependent anion channel (VDAC) and mitochondrial transcription factor A (TFAM; catalog nos. PA1–954A and PA5–68789, respectively; Thermo Fisher Scientific, Waltham, MA); Tom20 and Tim23 (catalog nos. 11802–1-AP and 11123–1-AP, respectively; Proteintech, Rosemont, IL); and nuclear respiratory factor 1 (NRF1), dynamin-related protein 1 (DRP1), phospho dynamin-related protein 1 (p-DRP1), p-AMPKα, and GAPDH (catalog nos. 46743, 8570, 4494, 4188, and 2118, respectively; Cell Signaling Technology, Danvers, MA). After several washes in Tris-buffered saline with Tween 20, membranes were incubated with appropriate peroxidase-conjugated secondary antibodies; bands were then visualized using enhanced chemiluminescence. For certain western blots (in Figures 2 and 5), the membrane was divided, and target proteins assessed on the respective sections of the membrane; GAPDH on this membrane was used to standardize these target proteins.

Assessment of Gene Expression
mRNA expression was assessed in cells and whole kidney tissues using a two-step quantitative real-time RT-PCR method as used in our previous studies (30,32). Briefly, RNA extraction was achieved using the TRIzol method (Invitrogen, Carlsbad, CA) with subsequent purification using a RNeasy Mini Kit (Qiagen, Valencia, CA). A Transcriptor First Strand cDNA Synthesis Kit (Roche Applied Science, Indianapolis, IN) was used for reverse transcription, and quantitative PCR was performed using TaqMan Gene Expression Assay sets (Applied Biosystems, Thermo Fisher Scientific) using standard curves constructed for the target and housekeeping genes. Results are reported as relative expression normalized to 18S rRNA.

NAD^+ and NADH Measurement
Measurement of NAD^+ and NADH content in whole kidney was performed using the NAD/NADH Assay Kit (catalog no. ab65348; Abcam) according to the manufacturer's instructions. Briefly, frozen whole kidney tissue was homogenized in 20 volumes of kit extraction buffer followed by centrifugation at 18,000 g for 3 minutes at 4°C. Supernatants were then passed through 10 kDa spin columns. Total NAD (NAD^+ and NADH) levels were assayed directly on these filtrates, and NADH levels were assessed in aliquots of the filtrates, which were heated at 60°C for 30 minutes to decompose NAD^+. NAD^+ and NADH content was normalized to tissue wet weight.

ATP Measurement

ATP content was measured in snap-frozen whole kidney tissue using a luminescence-based assay kit (catalog no. FLAA-1KT; Sigma–Aldrich, St. Louis, MO) according to the manufacturer's instructions. Briefly, kidney lysates were prepared by homogenization of tissues in ten volumes of ice-cold 2.5% TCA and centrifugation at 10,000 g for 10 minutes at 4°C. After adjusting the lysate pH to 7.86 with Tris base, and a second centrifugation to clear precipitation, ATP concentration was determined using a TD-20/20 luminometer (Turner Designs, Sunnyvale, CA). The precipitated pellets were resuspended in 0.5 N NaOH, and the protein content of each was determined using the BCA assay; ATP content was calculated as nanomoles of ATP per milligram of protein.

Ultrastructural Studies by Serial Block-face Scanning Electron Microscopy

Sham and HP-AKI-treated kidney samples for serial block-face scanning electron microscopy (SBF-SEM) were prepared using a protocol developed as described (33). Briefly, cortical tissue from sham and HP-AKI kidneys was dissected and fixed by immersion in 2% glutaraldehyde+2% paraformaldehyde in 0.1 M cacodylate buffer containing 2 mM calcium chloride. After fixation, samples were rinsed in 0.1 M cacodylate buffer and placed into 2% osmium tetroxide+1.5% potassium ferricyanide in 0.1 M cacodylate, washed with H_2O, incubated at 50°C in 1% thiocarbohydrazide, rinsed in H_2O, and placed in 2% uranyl acetate overnight. The next day, samples were rinsed again in H_2O, incubated with Walton's lead aspartate, dehydrated through an ethanol series, and embedded in Embed 812 resin.

To prepare embedded sample for placement into the SBF-SEM, a piece from the cortex area of sham and HP-AKI kidneys measuring around 1 mm^3 was trimmed of any excess resin and mounted to an 8-mm aluminum stub using silver epoxy Epo-Tek (EMS, Hatfield, PA). The mounted samples were then carefully trimmed into a smaller tower measuring around 0.5 mm^3 using a Diatome diamond trimming tool (EMS) and vacuum sputter-coated with gold palladium to help dissipate charge.

Sectioning and imaging of samples were performed using a VolumeScope 2 SEM (Thermo Fisher Scientific). Imaging was performed under high vacuum/low water conditions with a starting energy of 1.8 keV and beam current of 0.10 nA. Serial sections 60-nm thick were removed from the block, providing a final 10 nm×10 nm×60 nm spatial resolution to reveal mitochondrial ultrastructure within the proximal tubule epithelial cells as described (34).

Image analysis, including registration, segmentation, volume rendering, and visualization, was performed using ImageJ, Amira (Thermo Fisher Scientific), and Reconstruct (35) software packages.

Transmission Electron Microscopy

Cortical tissue from sham and HP-AKI kidneys was dissected and fixed using 4% paraformaldehyde+1% glutaraldehyde in 0.1 M phosphate buffer, pH 7.2 (PB). After fixation, the tissue was washed with PB, stained with 1% osmium tetroxide, washed in H_2O, stained in 2% uranyl acetate, washed in H_2O, dehydrated through a graded series of ethanol and acetone, and then embedded in Embed 812 resin. After a 24-hour polymerization at 60°C, 0.1 μM ultrathin sections were prepared and post stained with lead citrate. Micrographs were acquired using a JEOL 1400 Plus transmission electron microscope (JEOL, Inc., Peabody, MA) at 80 keV equipped with a Gatan Orius camera (Gatan, Inc., Warrendale, PA).

In Vitro Studies

Human renal proximal tubule epithelial cells (RPTECs) used in these studies were obtained from Lonza (Walkersville, MD) and used from passages 3 to 5. Additionally, murine RPTECs were isolated and cultured as described (34). Briefly, these cells were maintained at 37°C in 95% air and 5% carbon dioxide in REBM basal medium with SingleQuot supplements (catalog nos. CC-3191 and CC-4127, respectively; Lonza). In studies of heme exposure, human RPTECs and murine RPTECs were incubated in basal medium containing hemin (25 µM, catalog no. H651–9; Frontier Scientific, Logan, UT) for 8 hours. The cells were then harvested for the assessment of gene and protein expression as described.

Statistics

Data are expressed as the mean±SEM and were considered statistically significant at $P<0.05$. The t test was used for parametric data, and the Mann–Whitney U test was used for nonparametric data.

Results

Impaired Kidney and Mitochondrial Function in HP-AKI

Kidney function in mice with HP-AKI compared with sham mice was impaired as reflected by significantly increased serum creatinine and BUN at both 8 and 24 hours after HP-AKI (Supplementary Figure 1, A and B).

Mitochondrial function in HP-AKI was evaluated using three indices—whole kidney ATP content, NAD^+ content, and the $NAD^+/NADH$ ratio—all of which were significantly reduced at 8 hours after HP-AKI (Figure 1).

Mitochondrial Biogenesis in HP-AKI

Expression of proteins essential for mitochondrial biogenesis was evaluated at 8 and 24 hours after HP-AKI. PGC-1α levels were significantly reduced in HP-AKI mice at both time points (Figure 2A). PGC-1α activates nuclear encoded mitochondrial protein NRF1, the latter also decreased in expression in HP-AKI (Figure 2B). PGC-1α, along with NRF1, indirectly regulates mitochondrial DNA transcription by upregulating TFAM. TFAM protein expression was significantly reduced at 8 and 24 hours after HP-AKI (Figure 2C). Mitochondrial biogenesis is thus impaired at an early timepoint after HP-AKI.

This decreased expression of PGC-1α may reflect decreased NAD^+ content (23,24). The decreased PGC-1α expression cannot be ascribed to AMPK because its expression at 8 hours was not significantly altered (sham 1.18±0.28 versus HP-AKI 1.67±0.26, P=NS). However, PGC-1α expression is suppressed by inflammatory cytokines, and as
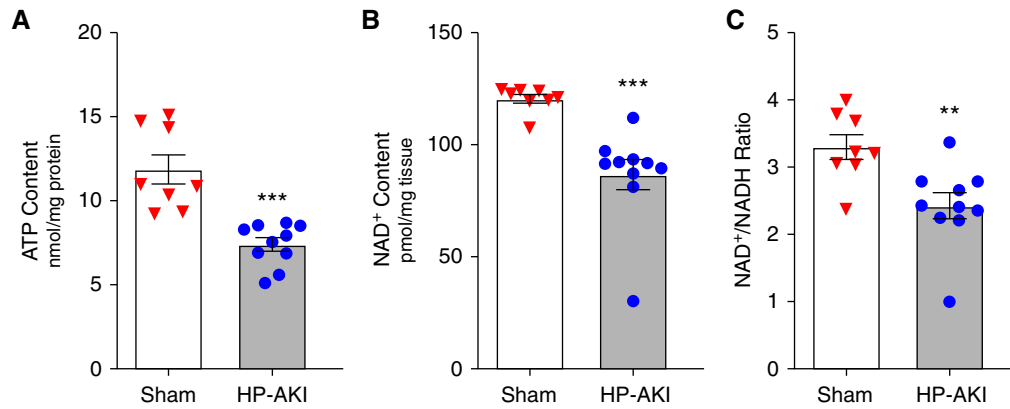
Figure 1. | Renal total ATP content, NAD$^+$ content, and NAD$^+$/NADH ratio in whole kidney of sham and heme protein–induced AKI (HP-AKI) mice. (A) Total ATP content was significantly reduced at 8 hours after HP-AKI compared with sham mice. (B) and (C) Total NAD$^+$ content and NAD$^+$/NADH ratio were significantly lower at 8 hours after HP-AKI compared with sham mice. $n=8$ and $n=10$ in sham and HP-AKI groups, respectively. ***$P<0.001$ and **$P<0.01$ versus sham group.

shown in Table 1, inflammatory cytokines are markedly upregulated in HP-AKI at 8 hours.

Mitochondrial Fission, Fusion, and Mitophagy in HP-AKI

Mitochondrial fission and fusion are tightly regulated in maintaining mitochondrial homeostasis. Mitochondrial fission fundamentally involves proteins such as DRP1. Renal p-DRP1(Ser616) levels were significantly increased at 8 and 24 hours after HP-AKI (Figure 3A). Renal DRP1 levels were also significantly increased at these time points after HP-AKI (Figure 3B).

Mitochondrial fusion compensates for and offsets mitochondrial fission as it enables the generation of larger, functional mitochondria. Mitochondrial fusion involves mitochondrial outer membrane proteins such as MFN2, among others. Renal MFN2 levels were significantly decreased at both 8 and 24 hours after HP-AKI (Figure 4A), indicating that HP-AKI also resulted in decreased mitochondrial fusion.

We assessed expression of PINK1 as a representative protein involved in mitophagy. PINK1 expression was significantly decreased at 24 hours after HP-AKI (Figure 4B).

Mitochondrial Outer and Inner Membrane Integrity in HP-AKI

VDAC is the most abundant outer membrane protein and is essential for mitochondrial integrity. VDAC protein expression was significantly decreased at 8 hours after HP-AKI (Figure 5A). The expression of another essential outer mitochondrial membrane protein, Tom20, was also significantly decreased at both 8 and 24 hours after
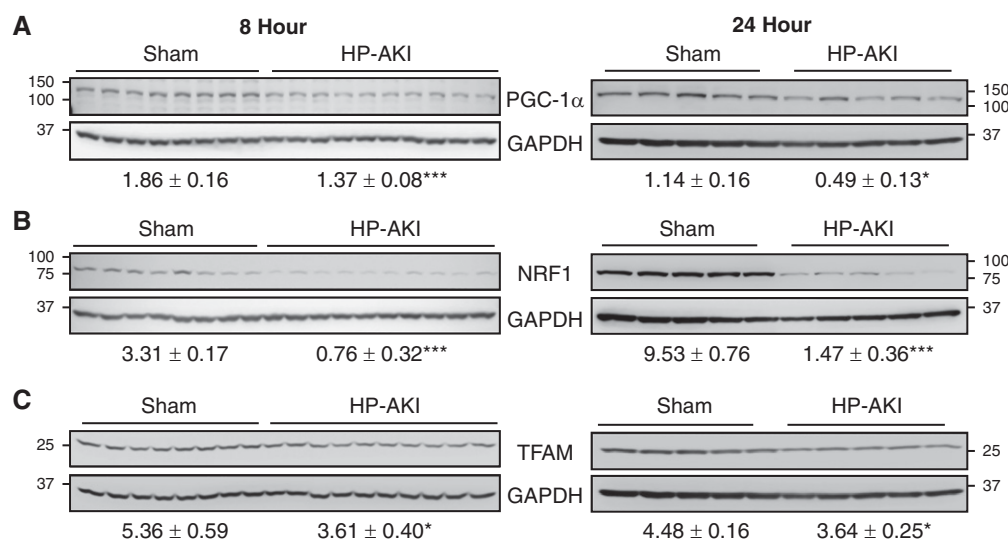

Figure 2. | Renal mitochondrial biogenesis in sham and HP-AKI mice. Expression of (A) peroxisome proliferator-activated receptor gamma coactivator-1α (PGC-1α), (B) nuclear respiratory factor 1 (NRF1), and (C) mitochondrial transcription factor A (TFAM) protein was significantly reduced at both 8 and 24 hours after HP-AKI compared with sham mice. Densitometry (mean±SEM), normalized for GAPDH expression, is displayed below blots. $n=8$ and $n=10$ in sham and HP-AKI groups, respectively, at 8 hours, and $n=5$ in each group at 24 hours. ***$P<0.001$ and *$P<0.05$ versus sham group. The 24-hour analyses of PGC-1α and TFAM were performed on the same membrane that was divided, as described in the Methods section. As such, the same GAPDH blot was employed for densitometric analysis for each of these targets and is displayed below both blots.

Table 1. Inflammatory gene expression in murine HP-AKI (8 hours)

Gene	Sham	HP-AKI	P Value
IL-6	4.6±1.1	483.3±156.7	0.008
TNF-α	3.6±0.2	7.7±1	<0.001
IL-1β	1.1±0.1	2.3±0.3	0.001
MCP-1	5.2±0.8	87.5±11.2	0.008
KC	3.7±0.2	731.2±51.2	<0.001
MMP-9	1.3±0.1	3.7±0.2	0.004
PAI-1	3.9±0.5	50.8±7	0.008

Real-time RT-PCR analysis normalized for 18S rRNA expression; $n=8$ and $n=10$ in sham and HP-AKI groups, respectively. HP-AKI, heme protein–induced AKI.

HP-AKI (Figure 5B). Expression of Tim23, an inner mitochondrial membrane protein, was reduced at 8 hours after HP-AKI (Figure 5C). A compensatory increase in synthesis may underlie the relative recovery of VDAC and TIM23 expression at 24 hours.

Mitochondrial Ultrastructure in HP-AKI

We examined mitochondrial ultrastructure in proximal tubule epithelial cells (PTECs) in the kidneys of sham and HP-AKI mice at 8 hours using SBF-SEM. Mitochondria were elongated and intact in PTECs in sham mice compared with relatively oval and rounded mitochondria with irregular and misshapen cristae in HP-AKI mice (Figure 6, A–D). In PTECs from HP-AKI mice, subsets of mitochondria were considerably swollen, whereas some mitochondria appeared smaller compared with cylindrically shaped mitochondria in sham kidneys (Figure 6, A–D). Morphometric studies from approximately 200 mitochondria from four different samples in each group demonstrated that the mean aspect ratio (major axis/minor axis) was significantly decreased in mitochondria from HP-AKI compared with mitochondria from sham kidneys (Figure 6E). Additionally, mitophagy was observed in HP-AKI (Supplementary Figure 2). Studies undertaken at 24 hours after HP-AKI demonstrate the presence of amorphous electron dense structures within mitochondria—findings indicative of irreversible cell injury (Supplementary Figure 3).

Three-dimensional imaging can provide conclusive evidence for fragmentation and fission of mitochondria, the latter not possible with 2D electron microscopy imaging. We thus undertook 3D reconstruction of the mitochondria on the basis of sixty, 60 nm serial sections from SBF-SEM images using Reconstruct software. Figure 7, C and D, display color-coordinated 3D reconstructed mitochondria that are also displayed in Figure 7, A and B, respectively. A representative section from sham and HP-AKI PTECs revealed intact, elongated mitochondria in sham kidneys, but relatively rounded and fragmented mitochondria in HP-AKI PTECs (Figure 7, C and D). Three-dimensional reconstruction thus conclusively demonstrates mitochondrial fragmentation and fission in HP-AKI.

Heme-mediated Mitochondrial Biogenesis and Fission *In Vitro*

As heme contributes to HP-AKI, *in vitro* studies were conducted to determine whether RPTECs exposed to heme recapitulate key features observed in HP-AKI *in vivo*. The mitochondrial biogenesis marker (PGC-1α) and mitochondrial fission marker (p-DRP1 and DRP1) were thus assessed. PGC-1α mRNA expression in heme-treated RPTECs was markedly decreased and was accompanied by striking induction of p-DRP1 protein expression, with no change in overall DRP1 protein expression (Figure 8). A possible basis for the marked suppression of PGC-1α is the robust proinflammatory effects of heme in RPTECs (Table 2).

Discussion

This study was predicated on two essential considerations: first, our prior observations in 1998 that demonstrated impaired mitochondrial respiration in this model of HP-AKI (22); and second, the need to evaluate in HP-AKI the novel concepts and pathways subsequently discovered in the intervening years regarding mitochondrial injury in AKI (23–27). To the best of our knowledge, this study is the first to undertake a comprehensive analysis of these
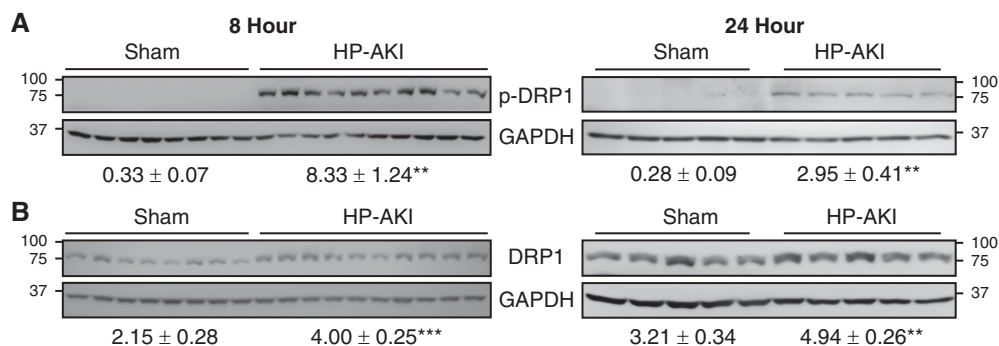

Figure 3. | Renal mitochondrial fission in sham and HP-AKI mice. Expression of (A) phospho dynamin-related protein 1 (p-DRP1) and (B) DRP1 protein was significantly increased at both 8 and 24 hours after HP-AKI compared with sham mice. Densitometry (mean±SEM), normalized for GAPDH expression, is displayed below blots. $n=8$ and $n=10$ in sham and HP-AKI groups, respectively, at 8 hours, and $n=5$ in each group at 24 hours. ***$P<0.001$ and **$P<0.01$ versus sham group.
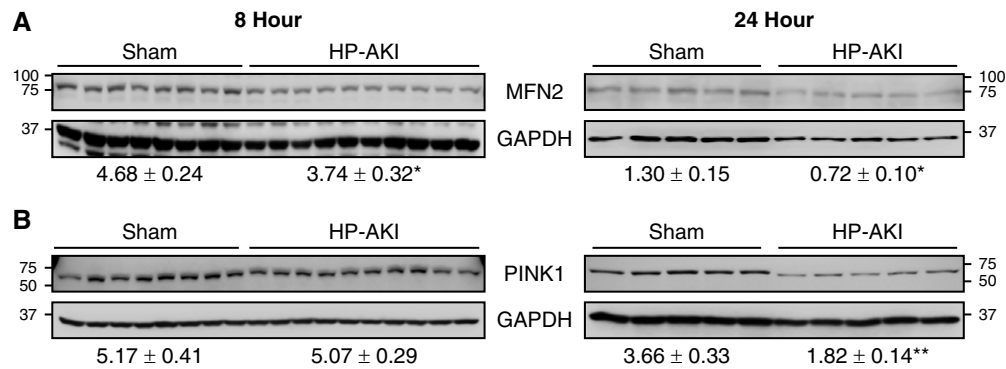
Figure 4. | **Renal mitochondrial fusion and mitophagy in sham and HP-AKI mice.** (A) Expression of mitochondrial fusion protein mitofusin 2 (MFN2) is decreased at both 8 and 24 hours after HP-AKI, whereas (B) expression of mitophagy-associated PTEN-induced kinase 1 (PINK1) protein is significantly reduced at 24 hours after HP-AKI compared with sham mice. Densitometry (mean±SEM), normalized for GAPDH expression, is displayed below blots. $n=8$ and $n=10$ in sham and HP-AKI groups, respectively, at 8 hours, and $n=5$ in each group at 24 hours. $**P<0.01$ and $*P<0.05$ versus sham group.

pathways in HP-AKI. We demonstrate the following regarding HP-AKI: (1) kidney content of ATP and NAD$^+$, which largely reflects mitochondrial function, is significantly reduced at a relatively early time point; (2) multiple biomarkers indicate impaired mitochondrial biogenesis; (3) proteins involved in mitochondrial fission are markedly upregulated, whereas those involved in mitochondrial fusion are downregulated; and (4) expression of mitochondrial proteins that maintain integrity of mitochondrial membranes is significantly reduced at an early time point.

Such impaired mitochondrial function and altered expression of these proteins are accompanied by profound changes in mitochondrial structure. First, mitochondria lose their cylindrical shape and become swollen and rounded, with significant separation and distortion of

mitochondrial cristae. Second, size heterogeneity exists with smaller mitochondria coexisting with swollen ones. Third, engulfing of injured mitochondria in autophagic vacuoles—mitophagy—was observed in some sections. Fourth, 3D analysis of mitochondria—indispensable in conclusively detecting mitochondrial fission and previously reported in IRI (34) but not in HP-AKI—demonstrated fragmentation and fission of mitochondria in HP-AKI. These 3D images of mitochondria are remarkably similar to mitochondrial images in prior seminal IRI studies (34). Our prior observations of human heme protein-AKI revealed mitophagy and prominent mitochondrial injury (36).

Our finding that PINK1 expression, a protein involved in mitophagy, was significantly decreased at 24 hours after HP-AKI merits comment. We offer four considerations in this
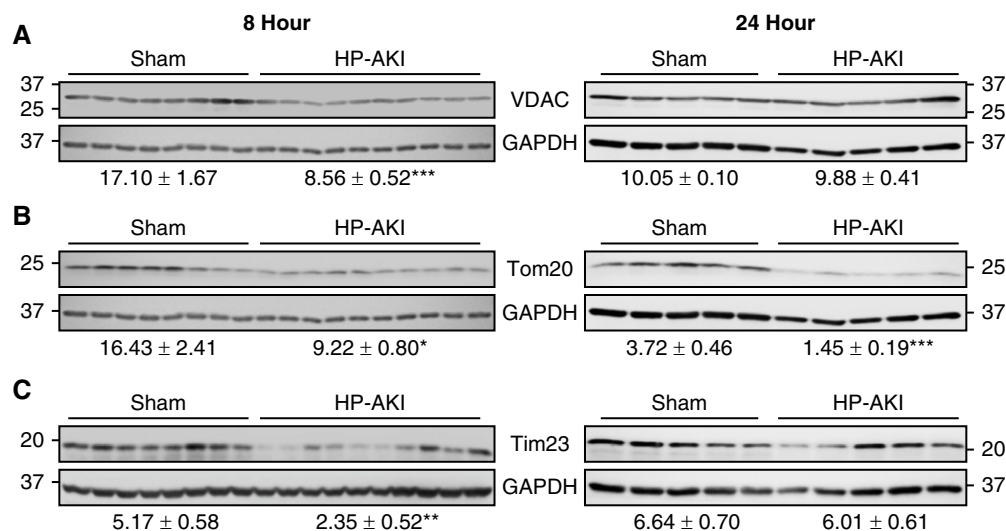

Figure 5. | **Renal mitochondrial membrane integrity in sham and HP-AKI mice.** Altered mitochondrial membrane integrity was observed at 8 and 24 hours after HP-AKI. (A) Decreased voltage-dependent anion channel (VDAC) protein expression was observed at 8 hours after HP-AKI, and (B) Tom20 protein expression was decreased at both 8 and 24 hours after HP-AKI. (C) Tim23 protein expression was significantly decreased at 8 hours after HP-AKI. Densitometry (mean±SEM), normalized for GAPDH expression, is displayed below blots. $n=8$ and $n=10$ in sham and HP-AKI groups, respectively, at 8 hours, and $n=5$ in each group at 24 hours. $***P<0.001$, $**P<0.01$, and $*P<0.05$ versus sham group. At each time point (8 and 24 hours), analyses of VDAC and Tom20 were performed on the same membrane that was divided, as described in the Methods section. At each time point, the same GAPDH blot was employed for densitometric analysis for each of these targets and is displayed below both blots.
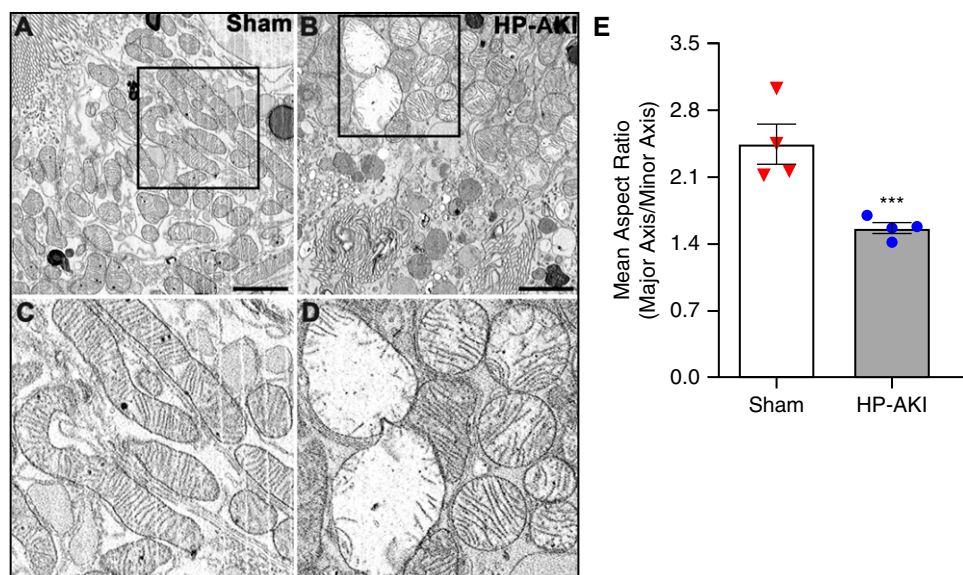
Figure 6. | **Mitochondrial ultrastructure in renal proximal tubules of sham and HP-AKI mice.** Electron microscopy revealed rounded mitochondria (B) in renal proximal tubule epithelial cells (RPTECs) at 8 hours after HP-AKI compared with elongated mitochondria in sham mice (A). (C) and (D) are higher magnifications of the insets in (A) and (B), respectively. (E) Morphometric assessment showed decreased mean aspect ratio (major axis length/minor axis length) of approximately 200 mitochondria from at least four different RPTECs from each group, indicating elongated mitochondria in sham group compared with relatively more rounded mitochondria in HP-AKI proximal tubules. Scale bar=5 μm; mean±SEM, ***$P<0.001$.

regard. First, proteins other than PINK1 are involved in mitophagy in AKI, and these may be more pertinent to HP-AKI (24,26,27). Second, the decreased PINK1 expression may be a maladaptive response. Third, the decreased PINK1

Figure 7. | **Three-dimensional reconstruction of mitochondria in renal proximal tubules of sham and HP-AKI mice.** (A) and (B) Representative serial section (of 60 sections imaged) from renal proximal tubules of sham and HP-AKI mice. Proximal tubules from sham mice displayed elongated mitochondria (A) compared with relatively more rounded mitochondria in HP-AKI proximal tubules (B). (C) and (D) Three-dimensional images were generated using Reconstruct software. Note the elongated mitochondria in sham mice compared with relatively rounded mitochondria and mitochondrial fission in HP-AKI mice.

expression may reflect consumption of the protein in mitophagy in the prior 24 hours. Fourth, in certain circumstances, PINK1 suppression may contribute to mitophagy (37).

NAD^+ is reduced in IRI and other types of AKI (24,26,27), but we are unaware of prior studies demonstrating such acute and early reduction in NAD^+ and the NAD^+/NADH ratio as we observed. The seminal insights by Parikh and colleagues demonstrating the beneficial effects of increased availability of NAD^+ in experimental AKI and that human AKI also exhibits evidence of impairment in net NAD^+ generation and content, in aggregate, support NAD^+-boosting strategies as a novel and feasible therapeutic strategy in AKI (4,5). Such a strategy is also relevant to HP-AKI, including, for example, AKI caused by rhabdomyolysis and by circulating CFH. CFH is increasingly recognized as a cause for sepsis-associated AKI and AKI after cardiopulmonary bypass (11). Additionally, CFH may contribute to AKI and CKD in sickle cell disease (38) and in pre-eclamptic states and the HELLP syndrome (39). Studies of NAD^+-boosting strategies in HP-AKI are thus of considerable interest.

Decreased NAD^+ content impairs ATP generation and reduces PGC-1α expression (24,26,27); the observed reduction in NAD^+ content in HP-AKI may thus account for the reduced ATP content and reduced expression of PGC-1α that were also observed. PGC-1α is a fundamental determinant of mitochondrial quality control in general and in fostering mitochondrial biogenesis in particular; adequate generation of ATP, essentially a mitochondrial-dependent function, thus critically depends on expression of PGC-1α. Older studies emphasize that reduced renal ATP content broadly sensitizes the kidney to acute insults (40). Accordingly, a positive feedback loop exists among these three molecules such that if the acute insult is severe enough, irrecoverable AKI may ensue. In addition to reduced
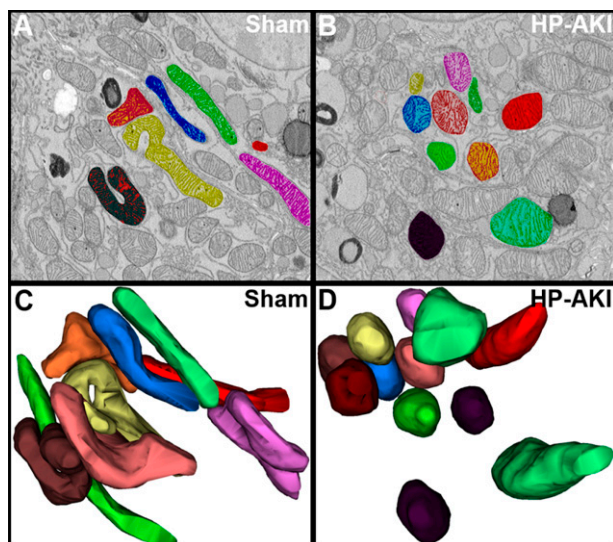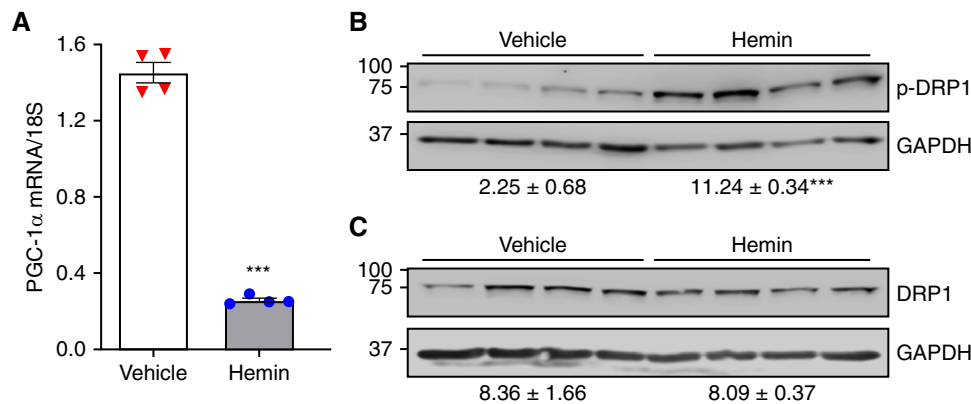
Figure 8. | Heme-mediated mitochondrial biogenesis and fission in human RPTECs. (A) Hemin treatment (25 μM, 8 hours) markedly decreased PGC-1α mRNA expression in human RPTECs as assessed by real-time RT-PCR analysis compared with vehicle treatment. Conversely, hemin treatment significantly increased p-DRP1 protein expression (B) with no change in overall DRP1 protein expression in human RPTECs (C) compared with vehicle treatment. Densitometry (mean±SEM), normalized for GAPDH expression, is displayed below blots. $n=4$ in each group. ***$P<0.001$ versus vehicle alone.

NAD$^+$ content, PGC-1α expression is strongly suppressed by inflammatory cytokines, and such an inflammatory response observed in HP-AKI may also contribute to the reduced PGC-1α expression in HP-AKI.

Increased intracellular heme occurs in HP-AKI as the kidney incorporates myoglobin and hemoglobin. Heme may also originate from destabilized heme proteins, in particular cytochrome p450, which are relatively unstable (20,41). Heme is prooxidant, proinflammatory, and proapoptotic (16,42,43). Intracellular heme impairs mitochondrial function; this effect is enabled by the intercalation of heme (a lipophilic molecule) in lipid-enriched mitochondrial membranes and the enhancement of the lipid-peroxidating effect of heme by the low-grade mitochondrial generation of hydrogen peroxide. We previously demonstrated that the exposure of normal mitochondria to concentrations of heme measured in mitochondria isolated from HP-AKI promptly impairs mitochondrial respiration (22). Accordingly, we examined the effects of heme on cellular expression of key representative molecules of mitochondrial biogenesis (PGC-1α) and mitochondrial fission (p-DRP1). Heme-exposed cells exhibited markedly reduced PGC-1α expression and robust induction of p-DRP1. We suggest that the increased

intracellular heme in HP-AKI contributes to the changes in these proteins observed in the kidney *in vivo* with HP-AKI. Heme also elicited a vigorous proinflammatory response *in vitro*; these findings are consistent with those observed *in vivo* and congruent with inflammation as a possible suppressor of PGC-1α expression.

In AKI, sublethal cell injury variably afflicts different cells. Analogously, various types of cell death may afflict different cells in AKI (44). The severity of sublethal cell injury and the type of cell death are not only site specific, but also may be dependent on the time point after AKI. Cell death caused by ferroptosis merits consideration because the kidney in HP-AKI exhibits several criteria that characterize ferroptosis, including lipid peroxidation, iron and ferritin buildup, impaired antioxidant mechanisms, and glutathione depletion (45,46). Ultrastructurally, ferroptosis exhibits mitochondrial fragmentation, with consistently smaller mitochondria, reduced number of cristae, and mitochondrial membrane densities. Some of these features were observed in some cells in HP-AKI.

Prior studies demonstrate that ATP in the kidney cortex is not significantly altered 24 hours after HP-AKI and that, at this time point, expression of PGC-1α is unaltered, whereas NRF-1 and TFAM are increased (47). Our present findings are in contrast to these prior studies in that we demonstrate an early reduction in ATP content within 8 hours, and at both 8 and 24 hours, expression of PGC-1α, NRF1, and TFAM is significantly reduced. The present findings are consistent with the profoundly impaired mitochondrial respiration we observed previously (22) and the ultrastructural damage observed in mitochondria in the present study, both of which would impair mitochondrial ATP-generating ability.

HP-AKI is a systemic disease with adverse effects directed to and away from the kidney: namely, released extrarenal nephrotoxins (myoglobin or hemoglobin) are delivered to and damage the kidney, and adverse effects of AKI then extend from the kidney to distant organs. A recent novel construct regarding AKI indicates that injured

Table 2. Inflammatory gene expression in murine RPTECs after 8 hours of heme treatment

Gene	Vehicle	Hemin	P Value
IL-6	8.2±0.7	16.8±0.7	<0.001
TNF-α	2.0±0.5	9.2±1.1	0.01
IL-1β	0.7±0.7	12.1±1.8	0.01
MCP-1	3.1±0.1	21.3±0.9	<0.001
KC	7.0±0.4	13.8±0.4	<0.001
MMP-9	2.4±0.1	8.2±0.4	0.008
PAI-1	7.0±0.4	40.9±1.5	0.008

Real-time RT-PCR analysis normalized for 18S rRNA expression; $n=4$ in each group. RPTECs, renal proximal tubule epithelial cells.

mitochondria are involved in mediating the adverse extra-renal effects of AKI (25). Danger-associated molecular patterns are released into the cytosol by injured mitochondria, thence into the circulation through the injured plasma membrane, and eventually conveyed to distant organs. This novel concept likely also applies to HP-AKI in view of the prominent mitochondrial injury in HP-AKI.

Prior studies of renal tubular function and morphology in HP-AKI demonstrate that the proximal tubule is severely injured, whereas aspects of distal tubular function (acidification and potassium secretion) are intact, but others are impaired (concentrating and diluting ability) (48). Examining distal nephron mitochondrial function and structure is of interest, and such studies are planned.

In conclusion, we demonstrate marked and early disturbances in mitochondrial dynamics as evidenced by exaggeration of pathways involved with mitochondrial fission in conjunction with impairment of pathways involved with mitochondrial biogenesis and fusion; ultrastructural derangements in mitochondria; and reduced NAD^+ and ATP content. Heme-exposed cells *in vitro* recapitulate two of these cardinal features: decreased and increased expression of PGC-1α and p-DRP1, respectively. The examination of the effects of NAD^+-boosting strategies and mitoprotective agents in HP-AKI is the basis for future investigations in HP-AKI.

Disclosures

C.M. Adams reports ownership interest in Emmyon, Inc.; research funding from Emmyon, Inc.; patents or royalties with Emmyon, Inc.; and an advisory or leadership role for Emmyon, Inc. J.P. Grande reports being a member of the editorial board for *Biochemistry and Molecular Biology Education Journal*. J.L. Kirkland reports ownership interest in Unity Biotechnologies. K.A. Nath reports an advisory or leadership role for *JASN* and *Mayo Clinic Proceedings*. T. Tchkonia reports ownership interest in Unity Biotechnology; honoraria from HRI Roswell Park Division and Pfizer; and patents or royalties from Unity Biotechnology. E. Trushina reports patents or royalties from the Mayo Clinic, and an advisory or leadership role for the National Institutes of Health Study Sections. All remaining authors have nothing to disclose.

Author Contributions

A.W. Ackerman, C.M. Adams, T.A. Christensen, A.J. Croatt, J.P. Grande, J.L. Kirkland, K.A. Nath, J.L. Salisbury, R.D. Singh, T. Tchkonia, and E. Trushina were responsible for validation; A.W. Ackerman, T.A. Christensen, A.J. Croatt, J.P. Grande, K.A. Nath, J.L. Salisbury, and R.D. Singh were responsible for data curation and formal analysis; A.W. Ackerman T.A. Christensen, A.J. Croatt, J.P. Grande, K.A. Nath, J.L. Salisbury, R.D. Singh, T. Tchkonia, and E. Trushina were responsible for the methodology; A.W. Ackerman, T.A. Christensen, A.J. Croatt, J.L. Kirkland, K.A. Nath, J.L. Salisbury, and R.D. Singh were responsible for resources; A.W. Ackerman, T.A. Christensen, A.J. Croatt, K.A. Nath, J.L. Salisbury, and R.D. Singh were responsible for visualization; A.W. Ackerman, A.J. Croatt, J.L. Kirkland, K.A. Nath, J.L. Salisbury, R.D. Singh, and E. Trushina were responsible for conceptualization; A.W. Ackerman, A.J. Croatt, K.A. Nath, J.L. Salisbury, and R.D. Singh were responsible for the software; A.W. Ackerman, A.J. Croatt, K.A. Nath, and R.D. Singh were responsible for the investigation and project administration and wrote the original draft of the manuscript; C.M. Adams, J.L. Kirkland, K.A. Nath, T. Tchkonia, and E. Trushina were responsible for funding acquisition; T.A. Christensen was responsible for the software; A.J. Croatt, K.A. Nath., and R.D. Singh were responsible for supervision; and all authors reviewed and edited the manuscript.

Data Sharing Statement

All data are included in the manuscript and/or supporting information.

Supplemental Material

This article contains the following supplemental material online at http://kidney360.asnjournals.org/lookup/suppl/doi:10.34067/KID.0004832022/-/DCSupplemental.

Supplementary Figure 1. Renal function in sham and heme protein–induced AKI (HP-AKI) mice.

Supplementary Figure 2. Mitophagy in renal proximal tubules of HP-AKI mice.

Supplementary Figure 3. Mitochondrial ultrastructure in renal proximal tubules of sham and HP-AKI mice using transmission electron microscopy (TEM).

References

1. Agarwal A, Dong Z, Harris R, Murray P, Parikh SM, Rosner MH, Kellum JA, Ronco C; Acute Dialysis Quality Initiative XIII Working Group: Cellular and molecular mechanisms of AKI. *J Am Soc Nephrol* 27: 1288–1299, 2016 https://doi.org/10.1681/ASN.2015070740

2. Silver SA, Chertow GM: The economic consequences of acute kidney injury. *Nephron* 137: 297–301, 2017 https://doi.org/10.1159/000475607

3. Nath KA: Models of human AKI: Resemblance, reproducibility, and return on investment. *J Am Soc Nephrol* 26: 2891–2893, 2015 https://doi.org/10.1681/ASN.2015101109

4. Poyan Mehr A, Tran MT, Ralto KM, Leaf DE, Washco V, Messmer J, Lerner A, Kher A, Kim SH, Khoury CC, Herzig SJ, Trovato ME, Simon-Tillaux N, Lynch MR, Thadhani RI, Clish CB, Khabbaz KR, Rhee EP, Waikar SS, Berg AH, Parikh SM: De novo NAD^+ biosynthetic impairment in acute kidney injury in humans. *Nat Med* 24: 1351–1359, 2018 https://doi.org/10.1038/s41591-018-0138-z

5. Ralto KM, Rhee EP, Parikh SM: NAD^+ homeostasis in renal health and disease. *Nat Rev Nephrol* 16: 99–111, 2020 https://doi.org/10.1038/s41581-019-0216-6

6. Gooch A, Westenfelder C: Modified hydrogels to enhance cellular therapy for AKI: A translational challenge. *J Am Soc Nephrol* 27: 2219–2221, 2016 https://doi.org/10.1681/ASN.2015121379

7. Fazekas B, Griffin MD: Mesenchymal stromal cell-based therapies for acute kidney injury: Progress in the last decade. *Kidney Int* 97: 1130–1140, 2020 https://doi.org/10.1016/j.kint.2019.12.019

8. Maines MD, Mayer RD, Ewing JF, McCoubrey Jr WK: Induction of kidney heme oxygenase-1 (HSP32) mRNA and protein by ischemia/reperfusion: Possible role of heme as both promotor of tissue damage and regulator of HSP32. *J Pharmacol Exp Ther* 264: 457–462, 1993

9. Agarwal A, Balla J, Alam J, Croatt AJ, Nath KA: Induction of heme oxygenase in toxic renal injury: A protective role in

cisplatin nephrotoxicity in the rat. *Kidney Int* 48: 1298–1307, 1995 https://doi.org/10.1038/ki.1995.414

10. Tracz MJ, Alam J, Nath KA: Physiology and pathophysiology of heme: Implications for kidney disease. *J Am Soc Nephrol* 18: 414–420, 2007 https://doi.org/10.1681/ASN.2006080894

11. Kerchberger VE, Ware LB: The role of circulating cell-free hemoglobin in sepsis-associated acute kidney injury. *Semin Nephrol* 40: 148–159, 2020 https://doi.org/10.1016/j.semnephrol.2020.01.006

12. Nath KA, Croatt AJ, Haggard JJ, Grande JP: Renal response to repetitive exposure to heme proteins: Chronic injury induced by an acute insult. *Kidney Int* 57: 2423–2433, 2000 https://doi.org/10.1046/j.1523-1755.2000.00101.x

13. Nath KA, Balla G, Vercellotti GM, Balla J, Jacob HS, Levitt MD, Rosenberg ME: Induction of heme oxygenase is a rapid, protective response in rhabdomyolysis in the rat. *J Clin Invest* 90: 267–270, 1992 https://doi.org/10.1172/JCI115847

14. Zarjou A, Bolisetty S, Joseph R, Traylor A, Apostolov EO, Arosio P, Balla J, Verlander J, Darshan D, Kuhn LC, Agarwal A: Proximal tubule H-ferritin mediates iron trafficking in acute kidney injury. *J Clin Invest* 123: 4423–4434, 2013 https://doi.org/10.1172/JCI67867

15. Guidet B, Shah SV: Enhanced *in vivo* H_2O_2 generation by rat kidney in glycerol-induced renal failure. *Am J Physiol* 257: F440–F445, 1989 https://doi.org/10.1152/ajprenal.1989.257.3.F440

16. Nath KA, Balla J, Croatt AJ, Vercellotti GM: Heme protein-mediated renal injury: A protective role for 21-aminosteroids *in vitro* and *in vivo*. *Kidney Int* 47: 592–602, 1995 https://doi.org/10.1038/ki.1995.75

17. Abul-Ezz SR, Walker PD, Shah SV: Role of glutathione in an animal model of myoglobinuric acute renal failure. *Proc Natl Acad Sci U S A* 88: 9833–9837, 1991 https://doi.org/10.1073/pnas.88.21.9833

18. Shah SV, Walker PD: Evidence suggesting a role for hydroxyl radical in glycerol-induced acute renal failure. *Am J Physiol* 255: F438–F443, 1988 https://doi.org/10.1152/ajprenal.1988.255.3.F438

19. Venkatachalam MA, Rennke HG, Sandstrom DJ: The vascular basis for acute renal failure in the rat. Preglomerular and postglomerular vasoconstriction. *Circ Res* 38: 267–279, 1976 https://doi.org/10.1161/01.RES.38.4.267

20. Baliga R, Zhang Z, Baliga M, Shah SV: Evidence for cytochrome P-450 as a source of catalytic iron in myoglobinuric acute renal failure. *Kidney Int* 49: 362–369, 1996 https://doi.org/10.1038/ki.1996.53

21. Van Avondt K, Nur E, Zeerleder S: Mechanisms of haemolysis-induced kidney injury. *Nat Rev Nephrol* 15: 671–692, 2019 https://doi.org/10.1038/s41581-019-0181-0

22. Nath KA, Grande JP, Croatt AJ, Likely S, Hebbel RP, Enright H: Intracellular targets in heme protein-induced renal injury. *Kidney Int* 53: 100–111, 1998 https://doi.org/10.1046/j.1523-1755.1998.00731.x

23. Clark AJ, Parikh SM: Mitochondrial metabolism in acute kidney injury. *Semin Nephrol* 40: 101–113, 2020 https://doi.org/10.1016/j.semnephrol.2020.01.002

24. Clark AJ, Parikh SM: Targeting energy pathways in kidney disease: The roles of sirtuins, AMPK, and PGC1α. *Kidney Int* 99: 828–840, 2021 https://doi.org/10.1016/j.kint.2020.09.037

25. Hepokoski M, Singh P: Mitochondria as mediators of systemic inflammation and organ cross talk in acute kidney injury. *Am J Physiol Renal Physiol* 322: F589–F596, 2022 https://doi.org/10.1152/ajprenal.00372.2021

26. Li Y, Hepokoski M, Gu W, Simonson T, Singh P: Targeting mitochondria and metabolism in acute kidney injury. *J Clin Med* 10: 3991, 2021 https://doi.org/10.3390/jcm10173991

27. Tang C, Cai J, Yin XM, Weinberg JM, Venkatachalam MA, Dong Z: Mitochondrial quality control in kidney injury and repair. *Nat Rev Nephrol* 17: 299–318, 2021 https://doi.org/10.1038/s41581-020-00369-0

28. Nath KA, Belcher JD, Nath MC, Grande JP, Croatt AJ, Ackerman AW, Katusic ZS, Vercellotti GM: Role of TLR4 signaling in the nephrotoxicity of heme and heme proteins. *Am J Physiol Renal Physiol* 314: F906–F914, 2018 https://doi.org/10.1152/ajprenal.00432.2017

29. Nath KA, Haggard JJ, Croatt AJ, Grande JP, Poss KD, Alam J: The indispensability of heme oxygenase-1 in protecting against acute heme protein-induced toxicity *in vivo*. *Am J Pathol* 156: 1527–1535, 2000 https://doi.org/10.1016/S0002-9440(10)65024-9

30. Nath KA, Singh RD, Grande JP, Garovic VD, Croatt AJ, Ackerman AW, Barry MA, Agarwal A: Expression of ACE2 in the intact and acutely injured kidney. *Kidney360* 2: 1095–1106, 2021 https://doi.org/10.34067/KID.0001562021

31. Singh RD, Barry MA, Croatt AJ, Ackerman AW, Grande JP, Diaz RM, Vile RG, Agarwal A, Nath KA: The spike protein of SARS-CoV-2 induces heme oxygenase-1: Pathophysiologic implications. *Biochim Biophys Acta Mol Basis Dis* 1868: 166322, 2022

32. Nath KA, Singh RD, Croatt AJ, Ackerman AW, Grande JP, Khazaie K, Chen YE, Zhang J: KLF11 is a novel endogenous protectant against renal ischemia-reperfusion injury. *Kidney360* 3: 1417–1422, 2022 https://doi.org/10.34067/KID.0002272022

33. Deerinck TJ, Shone TM, Bushong EA, Ramachandra R, Peltier ST, Ellisman MH: High-performance serial block-face SEM of nonconductive biological samples enabled by focal gas injection-based charge compensation. *J Microsc* 270: 142–149, 2018 https://doi.org/10.1111/jmi.12667

34. Brooks C, Wei Q, Cho SG, Dong Z: Regulation of mitochondrial dynamics in acute kidney injury in cell culture and rodent models. *J Clin Invest* 119: 1275–1285, 2009 https://doi.org/10.1172/JCI37829

35. Fiala JC: Reconstruct: A free editor for serial section microscopy. *J Microsc* 218: 52–61, 2005 https://doi.org/10.1111/j.1365-2818.2005.01466.x

36. Qian Q, Nath KA, Wu Y, Daoud TM, Sethi S: Hemolysis and acute kidney failure. *Am J Kidney Dis* 56: 780–784, 2010 https://doi.org/10.1053/j.ajkd.2010.03.025

37. Dagda RK, Cherra 3rd SJ, Kulich SM, Tandon A, Park D, Chu CT: Loss of PINK1 function promotes mitophagy through effects on oxidative stress and mitochondrial fission. *J Biol Chem* 284: 13843–13855, 2009 https://doi.org/10.1074/jbc.M808515200

38. Nath KA, Hebbel RP: Sickle cell disease: Renal manifestations and mechanisms. *Nat Rev Nephrol* 11: 161–171, 2015 https://doi.org/10.1038/nrneph.2015.8

39. Wester-Rosenlöf L, Casslén V, Axelsson J, Edström-Hägerwall A, Gram M, Holmqvist M, Johansson ME, Larsson I, Ley D, Marsal K, Mörgelin M, Rippe B, Rutardottir S, Shohani B, Akerström B, Hansson SR: A1M/α1-microglobulin protects from heme-induced placental and renal damage in a pregnant sheep model of preeclampsia. *PLoS One* 9: e86353, 2014 https://doi.org/10.1371/journal.pone.0086353

40. Nath KA, Norby SM: Reactive oxygen species and acute renal failure. *Am J Med* 109: 665–678, 2000 https://doi.org/10.1016/S0002-9343(00)00612-4

41. Paller MS, Jacob HS: Cytochrome P-450 mediates tissue-damaging hydroxyl radical formation during reoxygenation of the kidney. *Proc Natl Acad Sci U S A* 91: 7002–7006, 1994 https://doi.org/10.1073/pnas.91.15.7002

42. Kanakiriya SK, Croatt AJ, Haggard JJ, Ingelfinger JR, Tang SS, Alam J, Nath KA: Heme: A novel inducer of MCP-1 through HO-dependent and HO-independent mechanisms. *Am J Physiol Renal Physiol* 284: F546–F554, 2003 https://doi.org/10.1152/ajprenal.00298.2002

43. Gonzalez-Michaca L, Farrugia G, Croatt AJ, Alam J, Nath KA: Heme: A determinant of life and death in renal tubular epithelial cells. *Am J Physiol Renal Physiol* 286: F370–F377, 2004 https://doi.org/10.1152/ajprenal.00300.2003

44. Linkermann A, Chen G, Dong G, Kunzendorf U, Krautwald S, Dong Z: Regulated cell death in AKI. *J Am Soc Nephrol* 25: 2689–2701, 2014 https://doi.org/10.1681/ASN.2014030262

45. Ni L, Yuan Y, Wu X: Targeting ferroptosis in acute kidney injury. *Cell Death Dis* 13: 182, 2022 https://doi.org/10.1038/s41419-022-04628-9

46. Adedoyin O, Boddu R, Traylor A, Lever JM, Bolisetty S, George JF, Agarwal A: Heme oxygenase-1 mitigates ferroptosis

in renal proximal tubule cells. *Am J Physiol Renal Physiol* 314: F702–F714, 2018 https://doi.org/10.1152/ajprenal.00044.2017

47. Funk JA, Schnellmann RG: Persistent disruption of mitochondrial homeostasis after acute kidney injury. *Am J Physiol Renal Physiol* 302: F853–F864, 2012 https://doi.org/10.1152/ajprenal.00035.2011

48. Westenfelder C, Arevalo GJ, Crawford PW, Zerwer P, Baranowski RL, Birch FM, Earnest WR, Hamburger RK, Coleman RD, Kurtzman NA: Renal tubular function in glycerol-induced acute renal failure. *Kidney Int* 18: 432–444, 1980 https://doi.org/10.1038/ki.1980.156